# Computational Studies of Lithium Diisopropylamide Deaggregation

Alexander C. Hoepker and David B. Collum*

Department of Chemistry and Chemical Biology Baker Laboratory, Cornell University, Ithaca, New York 14853−1301, United States

S Supporting Information

ABSTRACT: Density functional theory computations [MP2/6-31G-(d)//B3LYP/6-31G(d)] on the deaggregation of lithium diisopropylamide (LDA) dimer solvated by two tetrahydrofuran ligands to give the corresponding trisolvated monomer show eight structurally distinct minima. The barriers to exchange are comparable to those expected from experimental studies showing rate-limiting deaggregations. The role of conformational isomerism in deaggregation and the extent that deaggregation rates dictate LDA reactivity under synthetically important conditions are considered.
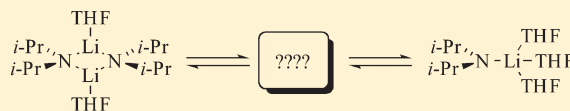
■ INTRODUCTION

Lithium diisopropylamide (LDA) is prominent in organic synthesis.[1] In a comprehensive survey of the frequency that reagents were used in approximately 500 natural product syntheses, LDA came out number one.[2] This prevalence is one of two reasons why we have focused on understanding the structure−reactivity relationships in LDA-mediated reactions. The other is that LDA offers a highly tractable template with which to study the influence of aggregation and solvation on organolithium reaction mechanisms.[3] The numerous synthetic applications of LDA combine with its complex coordination chemistry to produce considerable mechanistic variations.

To understand the source of the complexity, if not the complexity itself, we present Scheme 1, which summarizes the deaggregation of disolvated LDA dimer **1** to trisolvated monomer **6**. For many reactions, typically those that are conveniently monitored between 0 and −60 °C, the aggregates equilibrate very quickly compared to the rate of reaction being studied. Under conditions of fully established equilibria, all aggregates are available to react with the substrate, and studies have shown that many do.[3] During the course of our research we began to believe that a coherent picture of reactivity had emerged, which prompted us to summarize the results in a review.[3]

Recent rate studies, however, began to uncover aberrant behaviors that failed to follow conventional patterns. For example, during studies of imine metalations in which the relative reactivities spanned an approximate 60 000-fold range, the most reactive imine required that the reaction temperature be reduced to −78 °C (eq 1).[4] This was the first time that we had investigated the kinetics of an LDA-mediated metalation at −78 °C, and something odd happened: the loss of imine failed to follow a normal (first-order) decay, instead displaying a persistent linearity over the first two half-lives. We noted but largely ignored this observation.[4] Soon thereafter, odd substrate decays began appearing in disparate reactions including a host of ortholithiations[5−7] (such as eqs 2 and 3)[8] and even 1,4-additions of LDA to unsaturated esters (eq 4).[9] *All* shared two common traits: they were carried out using LDA in tetrahydrofuran (THF) at −78 °C, and they displayed hypersensitivities to traces of LiCl (as little as 1.0 ppm).
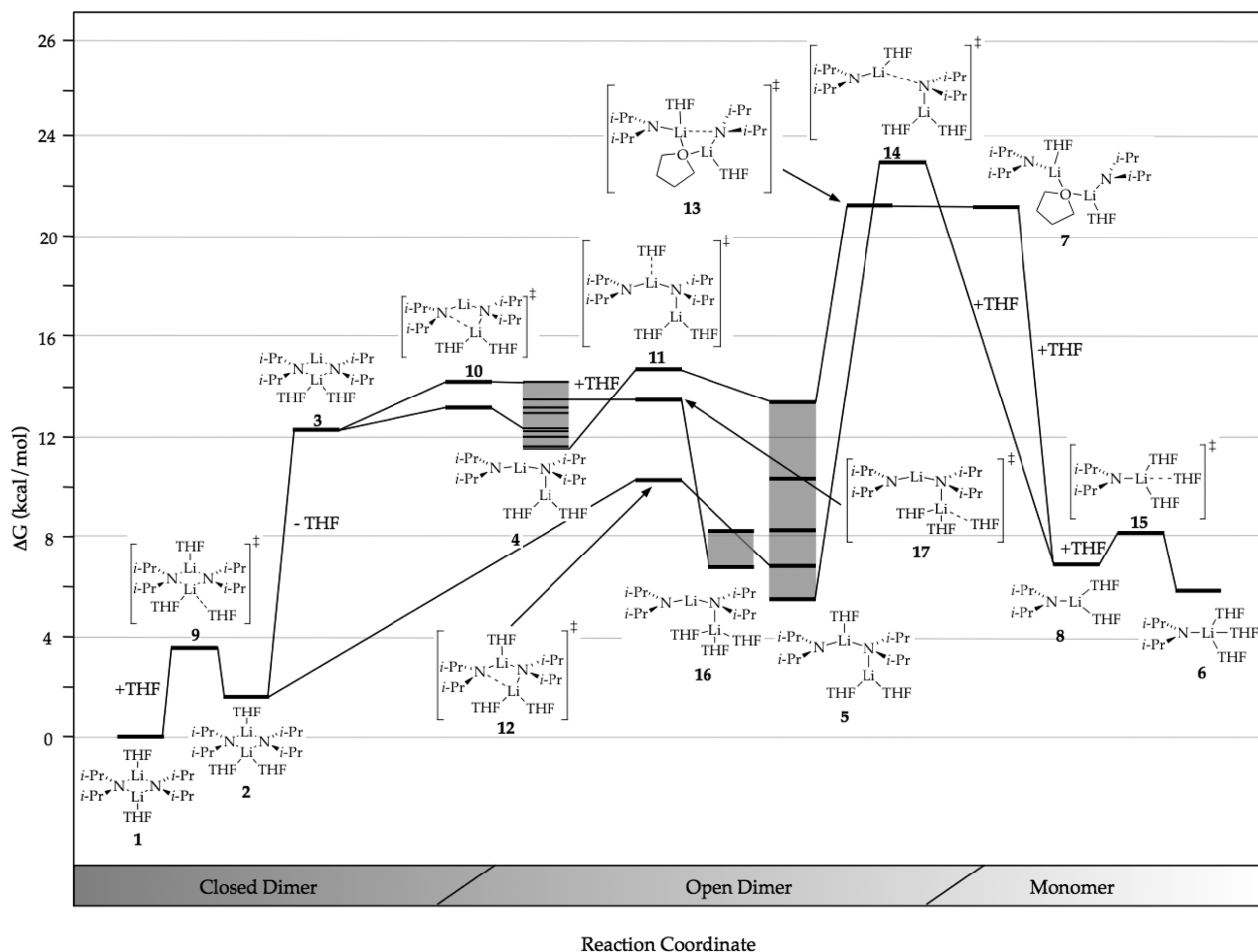

Scheme 1

Scheme 2

ΔG (kcal/mol)

Closed Dimer | Open Dimer | Monomer

Reaction Coordinate
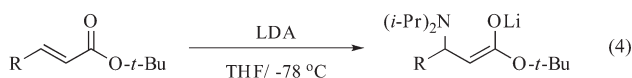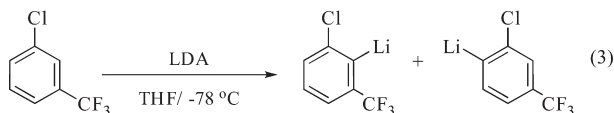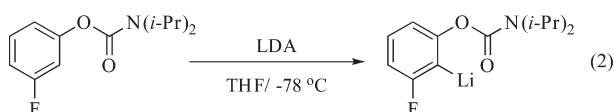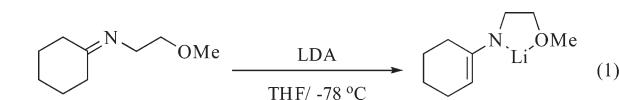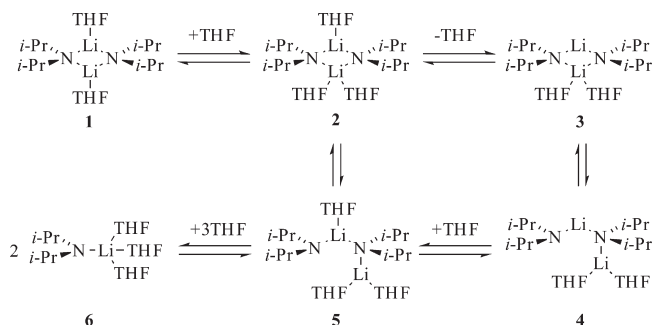
Mechanistic studies indicated that LDA aggregate exchanges were dictating the reaction rate,[10] causing the emerging mechanistic picture to be quite vexing. The odd linear decays observed for ortholithiations of aryl carbamates (eq 2), apparent zeroth-order substrate dependencies consistent with rate-limiting deaggregation of LDA dimer, were traced instead to virulent autocatalysis and the intervention of highly reactive mixed aggregates.[6] Unusual time-dependent changes in the concentration of LDA—ArLi mixed dimers attested to nonequilibrium conditions. The ortholithiation in eq 3 was found to be both autocatalyzed[11,12] and LiCl catalyzed, but the rate-limiting step of the uncatalyzed metalation involved rate-limiting deaggregation, a true zeroth-order substrate dependence, via a disolvated-dimer-based transition structure. Post-rate-limiting lithiation was shown to occur via a fleeting dimer-based rather than a monomer-based intermediate. Both autocatalysis and LiCl catalysis, by contrast, were shown to divert the reaction through a monomer-based mechanism. Seemingly analogous linear decays for 1,4-additions of LDA to unsaturated esters (eq 4) also involved a rate-limiting deaggregation of LDA, but it was found to occur via a *trisolvated*-dimer-based transition structure rather than via a disolvated dimer seen for ortholithiation.[9] Different substrates were reacting via different rate-limiting deaggregations! The post-rate-limiting 1,4-additions were shown to proceed via an LDA-monomer-based pathway. Highly muted autocatalysis and dramatic

catalysis by LiCl were traced explicitly to catalyzed deaggregation to the same LDA monomer.[13]

Although in isolation the case studies are logical, considered together they paint a chaotic mechanistic picture. We began to realize that a complete understanding of LDA-mediated reactions under these highly prevalent conditions, LDA/THF/ −78 °C, demand a more general and comprehensive understanding of LDA deaggregation. Although aggregation dynamics have received some attention, detailed analyses of organolithium deaggregations are absent.[14]

In this paper computational studies show that the intermediates in Scheme 1 are legitimate minima en route from the resting state of LDA (1)[15] to fleeting trisolvated monomer 6. Moreover, conformational effects on the stabilities of 1−6 as well as on the activation barriers to exchange are surprising in both detail and implication.[16]

### ■ RESULTS

General. All structures were computed using diisopropylamido groups and THF ligands without structural approximations. Density functional theory (DFT) and MP2 calculations were performed with the Gaussian 09 package using Gaussview 5.0 and WebMO as a graphical user interface.[17] Geometry optimizations and frequency calculations were performed at the B3LYP

level of theory using the 6-31G(d) and 6-31+G(d) Pople basis sets. Free energies were calculated from an MP2-derived single-point energy [6-31G(d) basis set] and a B3LYP-derived thermal correction [6-31G(d)] at 195 K (−78 °C) and 1 atm.[18] (MP2 corrections seem to provide superior correlations of theory and experiment, especially for the most highly solvated forms of LDA.)[19] Basis set superposition errors (BSSE)[20] were corrected using the counterpoise method[21] to test for energy errors arising from incomplete basis sets. Geometries that are particularly sensitive to BSSE will be discussed. Transition structures were confirmed by the existence of a single imaginary frequency, and intrinsic reaction coordinate (IRC) calculations[22] confirm the connection with specific minima. The energy surface describing LDA deaggregation is summarized in Scheme 2.

Minima. Moving from left to right in Scheme 2 corresponds to the stepwise conversion of known disolvated dimer **1**[15] (and related less symmetric cyclic dimers) through open dimers to give monomers as indicated in gray scale along the reaction coordinate (x axis). The key minima in Scheme 2 correspond to structures **1**−**6** in Scheme 1. Bridged dimer **7** and disolvated monomer **8** precede minima corresponding to monomer **6**. The shaded regions correspond to conformational ensembles of di- and trisolvated open dimers **4** and **5**.[23] Energy levels inside the shaded region correspond to distinct conformers. The lines illustrate connections between transition structures and specific conformational isomers of minima. Minima **2** and **3** are linked directly because the transformation is computed to be barrierless.

The steric demands and chirality of the isopropyl group render the potential energy surface of LDA aggregation and solvation rich in detail. Diisopropylamido moieties display two conformational minima corresponding to mirror images (eq 5).[24] Consequently, LDA dimers can exist as both homochiral and heterochiral (meso) diastereomers. A number of comparisons, however, show that in the open dimers and open dimer-based transition structures, the two diisopropylamido moieties do not communicate, resulting in comparable energies. The energies in Scheme 2 derive from the homochiral form. In the cyclic dimers (**1**, **2**, and **3**), the homochiral form is preferred over the heterochiral (meso) form by ≈1 kcal/mol. The computed structure of **1** matches the crystal structure.[15a]

$$(5)$$
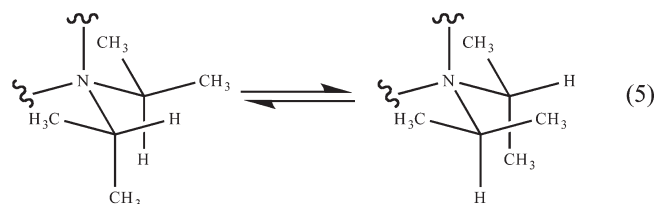
Two spatial relationships are prominent in open dimers. By sighting along the axis defined by the two nitrogen atoms (dashed line in Scheme 3), we loosely define a pseudo dihedral angle (ω_{CC}) to describe conformational isomerism arising from the rotational orientations of the two diisopropylamido moieties. These orientations are most easily envisioned by imagining rotation about the N−Li bond of the terminal diisopropylamido group. We define a second, standard dihedral angle (ω_{LiO}) that describes the THF orientations as defined by rotation about the N−Li bond to the terminal lithium. The open dimers are organized by dihedral angles ω_{CC} and ω_{LiO} in Supporting Information. Other minor conformational adjustments, such as

Scheme 3
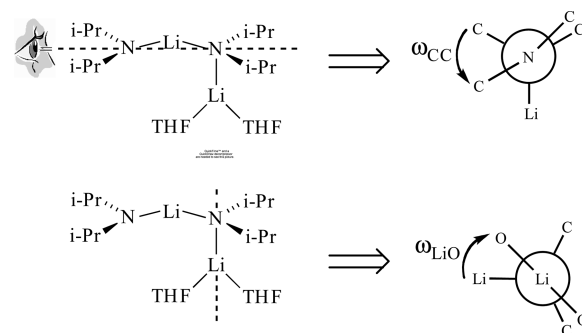
Scheme 4
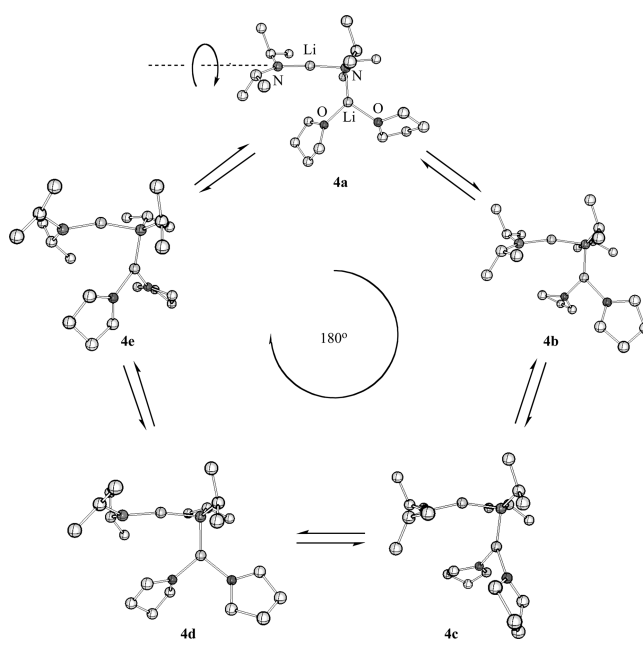
the rotations about the individual THF ligands, coincide with these primary conformational changes.

We sampled the conformers of disolvated open dimers **4** by incrementally varying ω_{CC}. Structures **4a**−**e** (Scheme 4) are representative of the eight conformers available through a 180° rotation, and they span a 2−3 kcal/mol range. (The three omitted do not include any exceptional structural features.) All conformers fall within an approximate 90° rotation. The conversion of **4e** to **4a** to complete the cycle requires an approximate 90° rotation of the diisopropylamido group, yet *no* minima are detectable. Changes in ω_{CC} are accompanied by changes in ω_{LiO} corresponding to seemingly fluid rotations about the THF-bearing N−Li bond that loosely approximate three orientations. We can find no simple (predictable) relationship between ω_{CC} and ω_{LiO}.

Analogous conformers are observed for trisolvated open dimers (Scheme 5), yet gearing arising from the high steric demands seems to allow for fewer minima at larger increments of ω_{CC}. The relative energies of the five conformers span an 8 kcal/mol range. All show a reduction of the N−Li−N angle to ≈165° owing to solvation of the internal lithium. The

conformers fit into three groups: (1) **5a** is unique in that the THF ligand on the interior lithium is orthogonal relative to the orientation in the other four conformers. Conformers **5b** and **5c** show evidence of diisopropylamido distortion and reduction of the Li—N—Li angle when compared with the disolvates that we attribute to buttressing. Conformers **5d** and **5e** seem most akin to the disolvated dimers in Scheme 4.

Transition Structures. Transition structures **9**—**15** connect select minima; dashed lines indicate bonds being cleaved. The transition structures are described by two fundamentally different imaginary vibrational modes: (1) Li—O stretching during THF dissociation/association, and (2) N—Li stretching during lithium amide bond formation/cleavage. Both modes are characterized by low absolute values in imaginary frequencies ranging from 18 to 49 cm^{-1}. The protocols required for locating transition structures are instructive. The standard method for locating transition structures was to perform a relaxed potential energy scan by incrementally stretching the bond of interest. For example, incrementally increasing the Li—O distance from 2.0 Å by steps of 0.1 Å raised the energy continuously until it dropped at 2.8 Å. Geometries were optimized at each point along the surface with the reaction coordinate describing the Li—O distance. The optimized geometry with r_{Li-O} = 2.8 Å was a good initial guess for a transition state optimization.

It became evident that only specific conformers could exit the trisolvated open dimer ensemble (Scheme 2). Whereas one conformer of **5** led to THF dissociation (**11**), another led to closed dimer formation (**12**), and two others led to fragmentation (**13** and **14**). The importance of sampling conformational space cannot be overstated. Transition structure **11** proved particularly difficult to locate but offered interesting insights. Incrementally stretching the Li—O bond afforded no saddle points starting from any of the four lowest-energy trisolvated open dimer conformers akin to **5**. Only by scanning from the highest-energy conformer could **11** finally be located. Incidentally, the highest-energy conformer connecting to **11** was not located by a rational sampling of all trisolvated open dimer conformers. A reverse IRC calculation from **13** led to this new geometry, which allowed us to locate **11**; serendipity played a big role. The strategy of palpating forward and backward along the reaction coordinate using output geometries as the input for a new search proved an important strategy for locating transition structures.

Transition structures corresponding to N—Li stretching (**10**, **12**, and **13**) were located using the scanning protocol. Again, the conformational geometry proved critical. Attempts to find transition structures describing the interconversion of conformers within the open dimer ensembles were unsuccessful, presumably owing to exceedingly low absolute values in the imaginary frequency. Casual inspection of the minima, however, suggests that their interconversion occurs via low energy barriers.

Tetrasolvated Open Dimers. There is no experimental support for tetrasolvated-dimer-based deaggregations of LDA, but thanks in large part to prompts by a referee we examined the viability of tetrasolvated minima and transition structures as illustrated in Scheme 6. The energies dovetail with those in Scheme 2. Trisolvated open dimer **5** binds a THF at the external lithium (**18**) while trisolvate **16** binds THF at the internal lithium (**19**), both yielding tetrasolvated open dimer **20**, albeit varying in conformational isomerism. Open dimer **20** then dissociates to two units of monomer **8** via transition structure **21** geometrically analogous to **13** and comparable in energy (22 kcal/mol).

Scheme 5
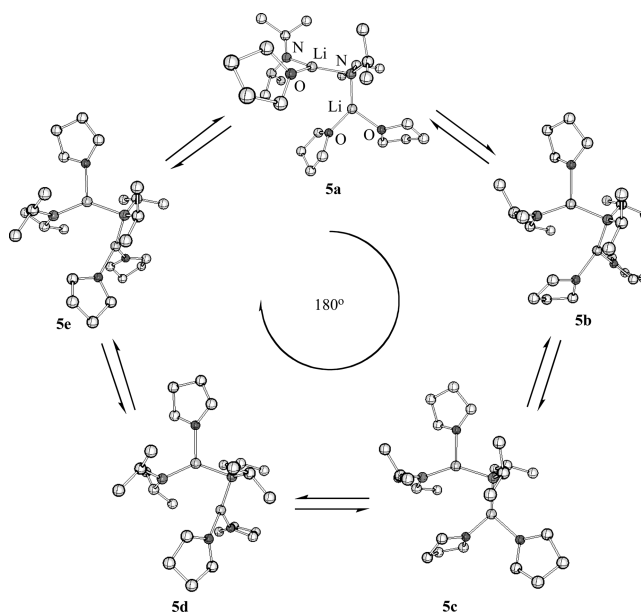
■ DISCUSSION

The experimental background presented in the Introduction paints a chaotic mechanistic picture of a delicate balance between rate-limiting aggregation events and rate-limiting reaction with substrates. DFT computational studies of LDA deaggregation afforded the series of minima that are illustrated in Scheme 1 and delineated in full detail with the accompanying transition structures in Scheme 2. The overall picture shows a series of fleeting intermediates and transition structures computed to be within an energy range commensurate with the activation energies of LDA-mediated metalations. The results for the di- and trisolvates reflect results stemming from detailed rate studies. In addition, we examined the role of tetrasolvate-based deaggregations, which are not (yet) experimentally documented (Scheme 6).

LDA Deaggregation: An Overview. The deaggregation of LDA dimer **1** is depicted moving from left to right along the reaction coordinate (x axis) of Scheme 2. Solvent exchanges interconverting closed dimers **1**—**3** are all facile, although asymmetric disolvate **3** is more than 12 kcal/mol less stable than dimer **1**. The N—Li bond scission affords either disolvated open dimer **4** from asymmetric disolvated dimer **3** or trisolvated open dimer **5** from **2**. Curiously, once open dimer **4** is formed, conversion to trisolvate **5** is a relatively unfavorable process. We elaborate on this finding in detail below.

The highest barriers in the conversion of LDA dimer **1** to monomer **6** result from the second N—Li bond scission. The direct cleavage of **5** via transition structure **14** is quite unfavorable. We suspected the requisite extrusion of a monosolvated monomer fragment is highly destabilizing. Consequently, we considered alternative transition structures in which one of the two THF ligands on the terminal lithium of **5** bridges the two lithiums (via **13**) to afford **7**. Computations show transition structure **13** to be preferred slightly over **14**. Dimer **7** is held together by a single bridging THF ligand and has exclusively three-coordinate lithiums. The role of bridging THFs has been mentioned previously in the context of deaggregations,[25] and

Scheme 6
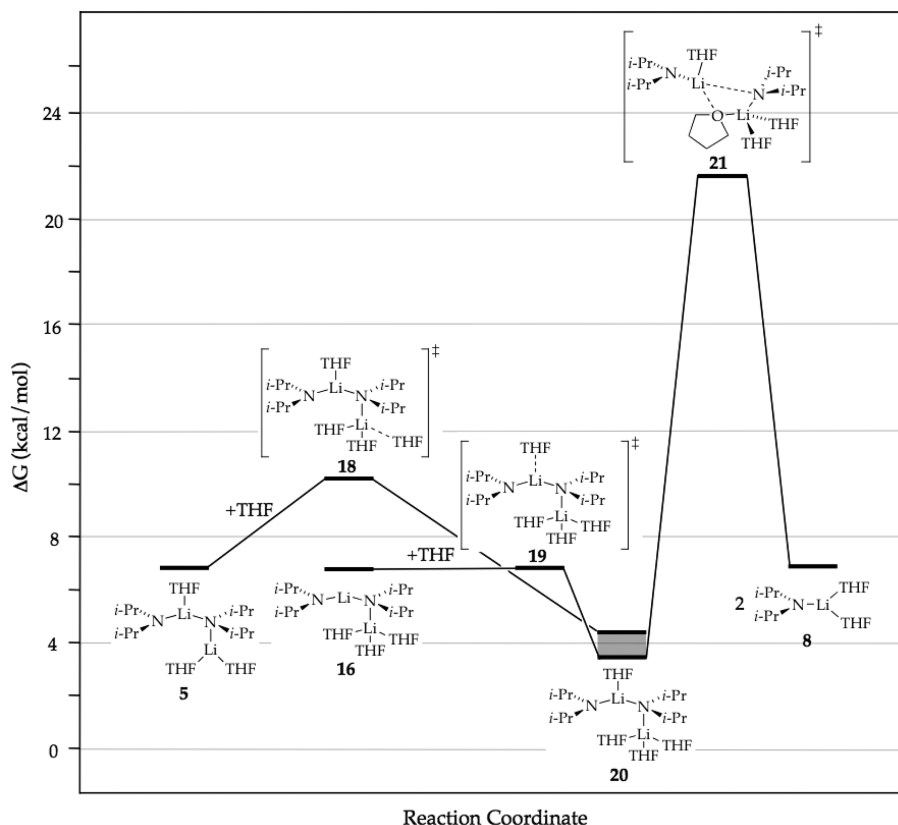
they are prevalent in the crystallographic literature.[26] We find the idea of such a neighboring-group-assisted scission as well as the symmetry of fleeting intermediate **13** to be appealing. Once extruded, disolvated LDA monomer **8** undergoes a facile solvation to give trisolvated monomer **6** as the most stable form.

Activation energies above 20 kcal/mol as computed for transition structures **13**, **14**, and **21** are disconcerting. We traced these high energies to the incomplete basis set of 6-31G(d). As we move from left to right along the reaction coordinate in Scheme 2, two originally intact N—Li bonds (**1**) are separated to a distance of around 3—5 Å. Whereas a fraction of the N—Li bond enthalpy remains, the low Pople basis set (mandated by the size of the structures) no longer captures this electron density overlap. This is widely recognized as the basis set superposition error (BSSE) and leads to increased energies.[20] Correcting for BSSE with the counterpoise method reduces the energy of **13** by ∼5 kcal/mol relative to **5**. (More details on the counterpoise calculation are in Supporting Information.) The energy of **13** relative to **5** is reduced using an increased basis set (B3LYP/aug-pVDZ), reaffirming that the high energies of structures akin to **13** are a consequence of an incomplete basis set. The energy of **13** is estimated to be a more realistic 16 kcal/mol.

The energies of transition structures with partially dissociated THF ligands (**9**, **11**, **12**, **15**, and **21**) also are elevated by about 2 kcal/mol resulting from BSSE. The effect of BSSE is especially pronounced as the O—Li distance is lengthened beyond 2.8 Å. Such is the case for **18** and **19**, which required an additional diffuse basis function [6-31+G(d)] for convergence of the transition state optimization.

Conformers and Portals. Both the cyclic dimers as well as the various transition structures are conformationally rigid, affording

two trivially different conformers; the cyclic dimers and transition structures are clearly *not* conformationally promiscuous. By contrast, open dimers **4** and **5** display inordinate conformational diversity. Rotation about the terminal diisopropylamido moiety in **4** by 180° (see ω_{CC} in Scheme 3) afford eight conformers spanning a 2—3 kcal/mol range; five of these conformers are illustrated in Scheme 4 and discussed in Results. The analogous survey of the more congested (highly geared) trisolvate **5** uncovered only five conformers spanning an 8 kcal/mol range (Scheme 5). An intriguing consequence of the conformationally variable open dimers and conformationally rigid transition structures is a notion we refer to as portals. In the most general sense, we find that the transition structures are flanked by a *single* conformer, a so-called portal, within the ensemble of conformers.

The specific example illustrated in Scheme 7 is instructive. The sequence begins with open dimer **4** in its most stable conformer (**4a**). IRC calculations confirm the conversion of conformer **4a** via transition structure **11** to give trisolvated open dimer as conformer **5a**. A particularly interesting point is noted by returning to Scheme 2. Conformer **4a** is the *lowest* energy conformer of **4**, whereas trisolvate **5a** is the *highest* energy conformer of **5**, *8 kcal/mol above the most stable conformer*. Even casual inspection of **5a** reveals an odd-looking orthogonal orientation of the THF ligand on the internal lithium when compared with the four other trisolvates illustrated in Scheme 5. To complete the deaggregation, **5a** is converted to dimer **7** via transition structure **13** involving N—Li bond scission with assistance by a bridging THF ligand. Dimer **7** is held together by a single bridging THF ligand, rendering it labile to solvent-assisted fragmentation to give monomer.

The conformational effects are more than idle curiosities; they could be the source of the complex and multifaceted dynamics of

Scheme 7
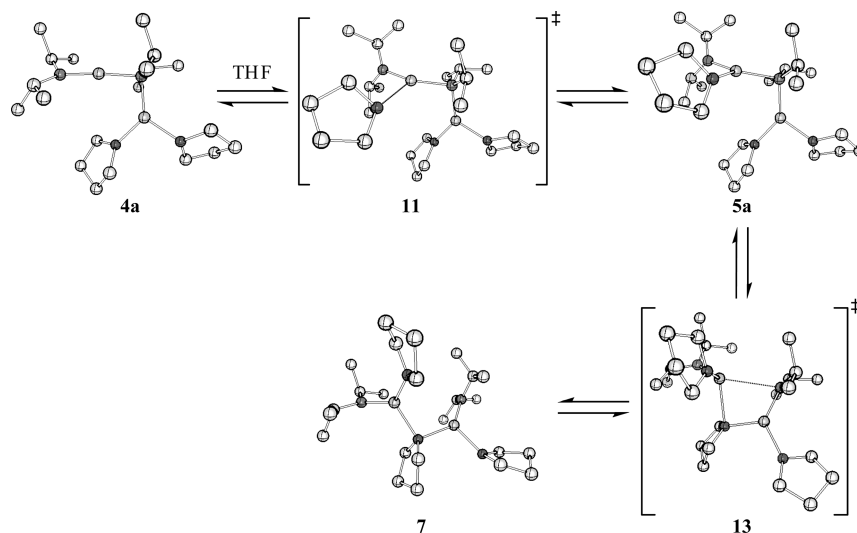
LDA. Direct conversion of disolvate **4** to trisolvate **5** is suggested to proceed through a very narrow conformational portal via a relatively higher energy transition structure **11** (Scheme 8). The computations indicate that the most expedient conversion of **4** to **5** is to return to starting dimer **1** (Scheme 8) and reopen via transition structure **12** to give trisolvate **5**.

Scheme 8
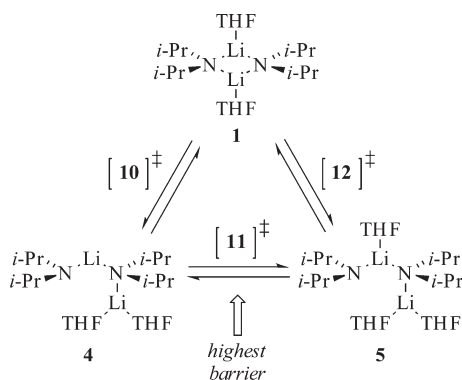
Rate-Limiting Deaggregations and Substrate Dependencies. The unequal receptivity of conformers of **4** to incoming ligands could be an important determinant of reactivity; pre-coordinating substrates, for example, would manifest a preference for particular conformers. Under conditions in which the subsequent reaction is fast on the time scale of substrate complexation (vide infra), coordination of substrate would be rate limiting and could be product determining.
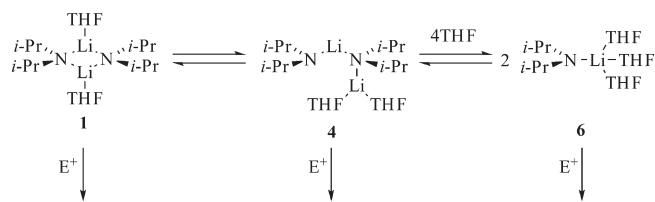
Mechanistic studies of LDA-mediated reactions in THF at −78 °C have focused on the role of rate-limiting deaggregation as well as ways in which salts catalyze and autocatalyze the deaggregation to form monomers. Throughout these studies, however, we have noted some odd behaviors including (1) rate-limiting deaggregations that proceed through transition structures of distinctly different stoichiometries (di- versus trisolvated dimers),[8,9,27a] (2) substrate-concentration-dependent rate-limiting deaggregations,[27a] (3) reactions following post-rate-limiting

steps that involve dimers and others that involve monomers,[27a] (4) reactions that are faster than those limited by aggregation and display substrate dependencies,[27] and (5) reactions in which proton transfers are *mechanistically* different than the corresponding deuterium transfers.[29] The computations serve as a pedagogically useful template with which to understand these seemingly disparate experimental observations.

Let us simplify the discussion by focusing on three structurally distinct forms of LDA (Scheme 9) and consider several discrete categories of reactivity:

(1) For the preponderance of LDA-mediated reactions studied to date,[3] the barriers to reactions with an electrophile, E^+, are measurably higher than the barriers to solvent and aggregate exchanges, which ensures that **1**, **4**, and **6** are at full equilibrium on the time scales of the reaction. Although one cannot say a priori which of the three will be the key intermediate from which the reaction occurs, the historical record suggests that reaction out of monomers is most likely.[3] Importantly, the *rates* that aggregation and solvation events occur do *not* dictate reaction rates.

(2) Imagine that the reactivity of E^+ is systematically increased with a commensurate decrease in reaction temperature to allow us to monitor the rates conveniently. At some level of reactivity, at some affiliated reaction temperature, the barrier to the formation of **6** is predicted to become higher than the barrier to reaction of E^+ with **1** or **4**. Through a bizarre twist of fate, that temperature is found experimentally to be approximately −78 °C, the most prevalent temperature reported by synthetic chemists. The reaction rate has become aggregation limited. Provided that monomer is the preferred pathway, then the rate-limiting transition structure is one of the trisolvated dimers **11**−**14**, which coincides nicely with rate studies of the 1,4-additions to unsaturated esters.[9] LiCl-catalyzed deaggregation (facile dimer−monomer equilibration) reduces the barrier to exchange, causing the reaction to become dependent once again on the structure and concentration of E^+. Catalysis and autocatalysis is prevalent for ortholithiations and 1,4-additions.

Scheme 9

Figure 1. Artist's rendition of acceleration by traces of lithium chloride (y axis) plotted versus the rate of the corresponding uncatalyzed metalation.

(3) With increasing reactivity of E[+], reaction via **4** becomes more viable. (In fact, reactions via all intermediates would be predicted to become more viable.) Even if monomers are extraordinarily reactive, reaction via dimer **4** will be observed if the barrier to deaggregation is too high. Fleeting dimer **4** could be formed reversibly, and the reaction would *still* be aggregation limited to the extent that access to monomer has been precluded. In such a scenario, the reaction with E[+] would be rate limiting and manifest a seemingly normal first-order substrate dependence. This scenario was noted during ortholithiations (eq 3).[8]

(4) Increasing the reactivity of the substrate in part 3 could cause **4** to be trapped efficiently on the time scales that **4** returns to cyclic dimer **1**. If so, the formation of dimer **4** becomes rate limiting. The reaction will display a zeroth-order in substrate, zeroth order in THF, and first order in LDA, all consistent with disolvated dimer **10** being the rate-limiting transition structure. The reaction would also, at least in principle, show no isotope effect. (We say more about isotope effects below.) Comparison of the two limiting scenarios in parts 3 and 4 shows that open dimer **4** can be cleanly rate limiting, partially rate limiting, or not rate limiting, all depending on the choice of substrate.[28]

(5) The most reactive substrates would find that the barrier to reaction with one of the closed dimers (**1**–**3**) is lower than the barrier to partial scission to form **4** or **5** and even lower than the free energies of **4** and **5**. Given the putative facile solvent exchange, these reactions would be faster than those that are aggregation limited. They would also exhibit first-order dependencies on E[+] and LDA concentrations as well as standard kinetic isotope effects. We have not documented uncontestable examples of facile reactions via closed dimers because the half-lives are quite short at −78 °C.[29] We have, however, obtained some hints of this behavior from ortholithiations, imine lithiations, and enolizations.[27c]

In a survey of the influence of catalytic quantities of LiCl on the rate of ortholithiation, we may have inadvertently scanned through the behaviors covered by parts 1–5. We offer a highly stylized graphic in Figure 1 to aid the description. We found that the least reactive substrates and the most reactive substrates were *not* catalyzed by LiCl, whereas substrates of intermediate reactivity displayed the properties of aggregate-limiting behavior consistent with the descriptions in parts 2–4.[7] These findings baffled us at the time but make sense in retrospect. Of course, the least reactive substrates lithiate under conditions of full aggregate equilibration (part 1), which eliminates the need for LiCl catalysis in the deaggregation. The most reactive substrates do not benefit from deaggregation because the free energy of formation of monomer is higher than the dimer-based transition structure (part 5). It is only those of intermediate reactivity for
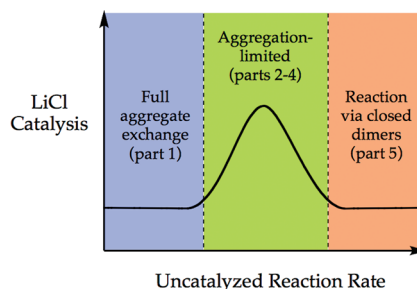
which catalysis of monomer formation can reduce the barrier of a beneficial (possibly mandatory) deaggregation (parts 2–4).

We close with some comments about kinetic isotope effects. Of course, a reaction in which proton transfer is rate limiting would manifest a primary kinetic isotope effect. In theory, a zeroth-order substrate dependence arising from a rate-limiting deaggregation would afford an isotope effect of unity. In practice, we have found that kinetic isotope effects above 30 are commonplace for ortholithiations, can cause the rate-limiting step to shift from deaggregation to deuterium transfer. This shift in rate limitation is, although complicating at times, quite logical.[27b]

■ CONCLUSION

We are struggling to understand a mechanistically complex subset of LDA chemistry in which aggregation events dictate reactivity. DFT computations describing the deaggregation of LDA dimer **1** to monomer **6** offer a number of potentially interesting qualitative and semiquantitative insights. The computed barriers for partial and total scission are comparable to the barriers gleaned from a growing body of experimentally derived examples of aggregation-limited reactions of LDA in THF at −78 °C. Although conformational isomerism of key intermediates (especially the most conformationally flexible open dimers) was expected, the number of minima and the range of their computed energies were certainly not. The most interesting aspect is that conformationally rigid transition structures serve as portals connecting specific conformers of open dimer intermediates. The conformational restrictions contribute to experimentally important activation barriers. The summaries in Schemes 1 and 2 offer excellent structural supports for discussions of seemingly disparate, sometimes paradoxical, experimental observations.

The complexity is exacerbated by lithium salt-catalyzed dimer–monomer exhange.[7] We have had some success examining the mechanism of catalysis, but the details of the underlying LDA–LiX interactions are still elusive. We also have unpublished data suggesting that conversions of cyclic dimers to open dimers are catalyzed, and that LDA-derived *tetramers* are central to some reactions.[27] Tetramer intermediates significantly change the plotline and add to the growing demand for a detailed experimental investigation of the solution dynamics of LDA in THF.

Of course, the experimental and computational conclusions apply only to reactions in THF solution. What happens when reactions are carried out in inferior ligands such as diethyl ether or *tert*-butyl methyl ether? Are rate-limiting deaggregations and salt-catalyzed deaggregations more or less prominent? We hope to pursue further studies.

■ ASSOCIATED CONTENT

S **Supporting Information.** Computational data including Cartesian coordinates and a complete list of authors for ref 17. This material is available free of charge via the Internet at http://pubs.acs.org.

■ AUTHOR INFORMATION

Corresponding Author
*E-mail: dbc6@cornell.edu.

■ ACKNOWLEDGMENT

■ REFERENCES

(1) (a) Bakker, W. I. I.; Wong, P. L.; Snieckus, V. Lithium Diisopropylamide. In *e-EROS*; Paquette, L. A., Ed.; Wiley: New York, 2001. (b) Clayden, J. *Organolithiums: Selectivity for Synthesis*; Baldwin, J. E., Williams, R. M., Eds.; Pergamon Press: New York, 2002. (c) Hartung, C. G.; Snieckus, V. In *Modern Arene Chemistry*; Astruc, D. Ed.; Wiley-VCH, Weinheim, 2002; Chapter 10.

(2) A survey was compiled by H. J. Reich and co-workers, unpublished.

(3) Collum, D. B.; McNeil, A. J.; Ramirez, A. *Angew. Chem., Int. Ed.* **2007**, *46*, 3002.

(4) Liao, S.; Collum, D. B. *J. Am. Chem. Soc.* **2003**, *125*, 15114.

(5) Singh, K. J.; Collum, D. B. *J. Am. Chem. Soc.* **2006**, *128*, 13753.

(6) Singh, K. J.; Hoepker, A. C.; Collum, D. B. *J. Am. Chem. Soc.* **2008**, *130*, 18008.

(7) Gupta, L.; Hoepker, A. C.; Singh, K. J.; Collum, D. B. *J. Org. Chem.* **2009**, *74*, 2231.

(8) Hoepker, A. C.; Gupta, L.; Ma, Y.; Faggin, M. F.; Collum, D. B. *J. Am. Chem. Soc.* **2011**, *133*, 7135.

(9) Ma, Y.; Hoepker, A. C.; Gupta, L.; Faggin, M. F.; Collum, D. B. *J. Am. Chem. Soc.* **2010**, *132*, 15610.

(10) For examples of reactions that are fast relative to the rates of aggregate−aggregate exchanges, see: (a) McGarrity, J. F.; Ogle, C. A. *J. Am. Chem. Soc.* **1985**, *107*, 1810. (b) Jones, A. C.; Sanders, A. W.; Bevan, M. J.; Reich, H. J. *J. Am. Chem. Soc.* **2007**, *129*, 3492. (c) Thompson, A.; Corley, E. G.; Huntington, M. F.; Grabowski, E. J. J.; Remenar, J. F.; Collum, D. B. *J. Am. Chem. Soc.* **1998**, *120*, 2028. (d) Jones, A. C.; Sanders, A. W.; Sikorski, W. H.; Jansen, K. L.; Reich, H. J. *J. Am. Chem. Soc.* **2008**, *130*, 6060.

(11) (a) Besson, C.; Finney, E. E.; Finke, R. G. *J. Am. Chem. Soc.* **2005**, *127*, 8179. (b) Besson, C.; Finney, E. E.; Finke, R. G. *Chem. Mater.* **2005**, *17*, 4925. (c) Huang, K. T.; Keszler, A.; Patel, N.; Patel, R. P.; Gladwin, M. T.; Kim-Shapiro, D. B.; Hogg, N. *J. Biol. Chem.* **2005**, *280*, 31126. (d) Huang, Z.; Shiva, S.; Kim-Shapiro, D. B.; Patel, R. P.; Ringwood, L. A.; Irby, C. E.; Huang, K. T.; Ho, C.; Hogg, N.; Schechter, A. N.; Gladwin, M. T. *J. Clin. Invest.* **2005**, *115*, 2099. (e) Tanj, S.; Ohno, A.; Sato, I.; Soai, K *Org. Lett.* **2001**, *3*, 287. (f) Barrios-Landeros, F.; Carrow, B. P.; Hartwig, J. F. *J. Am. Chem. Soc.* **2008**, *130*, 5842.

(12) (a) Depue, J. S.; Collum, D. B. *J. Am. Chem. Soc.* **1988**, *110*, 5524. (b) McNeil, A. J.; Toombes, G. E. S.; Gruner, S. M.; Lobkovsky, E.; Collum, D. B.; Chandramouli, S. V.; Vanasse, B. J.; Ayers, T. A. *J. Am. Chem. Soc.* **2004**, *126*, 16559. (c) Nudelman, N. S.; Velurtas, S.; Grela, M. A. *J. Phys. Org. Chem.* **2003**, *16*, 669. (d) Alberts, A. H.; Wynberg, H. *J. Am. Chem. Soc.* **1989**, *111*, 7265. (e) Alberts, A. H.; Wynberg, H. *J. Chem. Soc., Chem. Commun.* **1990**, 453.

(13) (a) Seebach, D. In *Proceedings of the Robert A. Welch Foundation Conferences on Chemistry and Biochemistry*; Wiley: New York, 1984; p 93. (b) Seebach, D. *Angew. Chem., Int. Ed. Engl.* **1988**, *27*, 1624. (c) Tchoubar, B.; Loupy, A. *Salt Effects in Organic and Organometallic Chemistry*; VCH: New York, 1992; Chapters 4, 5, and 7. (d) Caubère, P. *Chem. Rev.* **1993**, *93*, 2317.

(14) For representative examples, see: (a) Arvidsson, P. I.; Ahlberg, P.; Hilmersson, G. *Chem.—Eur. J.* **1999**, *5*, 1348. (b) Fraenkel, G.; Henrichs, M.; Hewitt, J. M.; Su, B. M.; Geckle, M. J. *J. Am. Chem. Soc.* **1980**, *102*, 3345. (c) Heinzer, J.; Oth, J. F. M.; Seebach, D. *Helv. Chim. Acta* **1985**, *68*, 1848. (d) Hilmersson, G.; Arvidsson, P. I.; Davidsson, Ö; Håkansson, M. *Organometallics* **1997**, *16*, 3352. (e) Hilmersson, G.; Davidsson, Ö. *Organometallics* **1995**, *14*, 912. (f) Fraenkel, G.; Fraenkel, A. M.; Geckle, M. J.; Schloss, F. *J. Am. Chem. Soc.* **1979**, *101*, 4745. (g) Fraenkel, G.; Chow, A.; Winchester, W. R. *J. Am. Chem. Soc.* **1990**, *112*, 6190.

(15) (a) Williard, P. G.; Salvino, J. M. *J. Org. Chem.* **1993**, *58*, 1. (b) Kim, Y.-J.; Bernstein, M. P.; Galiano-Roth, A. S.; Romesberg, F. E.; Fuller, D. J.; Harrison, A. T.; Collum, D. B.; Williard, P. G. *J. Org. Chem.* **1991**, *56*, 4435.

(16) (a) Pratt, L. M. *THEOCHEM* **2007**, *811*, 191. (b) Pratt, L. M. *Bull. Chem. Soc. Jpn.* **2005**, *78*, 890. (c) Pratt, L. M.; Newman, A.; Cyr, J. S.; Johnson, H.; Miles, B.; Lattier, A.; Austin, E.; Henderson, S.; Hershey, B.; Lin, M.; Balamraju, Y.; Sammonds, L.; Cheramie, J.; Karnes, J.; Hymel, E.; Woodford, B.; Carter, C. *J. Org. Chem.* **2003**, *68*, 6387. (d) Armstrong, D. R.; Carstairs, A.; Henderson, K. W. *Organometallics* **1999**, *18*, 3589. (e) Romesberg, F. E.; Collum, D. B. *J. Am. Chem. Soc.* **1995**, *117*, 2166. (f) Romesberg, F. E.; Collum, D. B. *J. Am. Chem. Soc.* **1994**, *116*, 9187. (g) Bernstein, M. P.; Romesberg, F. E.; Fuller, D. J.; Harrison, A. T.; Williard, P. G.; Liu, Q. Y.; Collum, D. B. *J. Am. Chem. Soc.* **1992**, *114*, 5100. Romesberg, F. E.; Collum, D. B. *J. Am. Chem. Soc.* **1992**, *114*, 2112. (h) Also see refs 5, 9, and 19.

(17) Frisch, M. J.; et al. *GaussianVersion 3.09*; revision A.1; Gaussian, Inc.: Wallingford, CT, 2009.

(18) The computations use the Gaussian standard state of 1.0 atm. If the THF concentration is corrected to neat THF (approximately 13 M), each solvation step benefits from approximately 2.0 kcal/mol of additional stabilization at −78 °C (195 K). Pratt, L. M.; Merry, S.; Nguyen, S. C.; Quan, P.; Thanh, B. T. *Tetrahedron* **2006**, *62*, 10821.

(19) The benefits of MP2 corrections in the context of higher solvates were specifically pointed out by an anonymous referee: Viciu, M.; Gupta, L.; Collum, D. B. *J. Am. Chem. Soc.* **2010**, *132*, 6361.

(20) (a) Jansen, H. B.; Ros, P. *Chem. Phys. Lett.* **1969**, *3*, 140. (b) Liu, B.; McLean, A. D. *J. Chem. Phys.* **1973**, *59*, 4557.

(21) Boys, S. F.; Bernardi, F. *Mol. Phys.* **1970**, *19*, 553.

(22) For a discussion of intrinsic reaction coordinate (IRC) calculations, see: Foresman, J. B.; Frisch, A. E. *Exploring Chemistry with Electronic Structure Methods*, 2nd ed.; Gaussian, Inc.: Pittsburgh, 1993.

(23) (a) Open dimers were first proposed for the isomerization of oxiranes to allylic alcohols by mixed metal bases. See: Mordini, A.; Rayana, E. B.; Margot, C.; Schlosser, M. *Tetrahedron* **1990**, *46*, 2401. (b) For a bibliography of lithium amide open dimers, see: Ramirez, A.; Sun, X.; Collum, D. B. *J. Am. Chem. Soc.* **2006**, *128*, 10326 and references cited therein.

(24) For leading references to conformational studies of diisopropylamino fragments, see: (a) Stewart, W. E.; Siddall, T. H. *Chem. Rev.* **1970**, *70*, 517. (b) Lidén, A.; Roussel, C.; Liljefors, T.; Chanon, M.; Carter, R. E.; Metzger, J.; Sandström, J. *J. Am. Chem. Soc.* **1976**, *98*, 2853.

(25) Clegg, W.; Horsburgh, L.; Mackenzie, F. M.; Mulvey, R. E. *J. Chem. Soc., Chem. Commun.* **1995**, 2011.

(26) Representative examples of structurally characterized bridging THF ligands: (a) Pratt, L. M.; Merry, A.; Nguyen, S. C.; Quanb, P.; Thanh, B. T. *Tetrahedron* **2006**, *62*, 10821. (b) Clegg, W.; Liddle, S. T.; Mulvey, R. E.; Robertson, A. *Chem. Commun.* **1999**, 511. (c) Boche, G.; Boie, C.; Bosold, F.; Harms, K.; Marsch, M. *Angew. Chem., Int. Ed.* **1994**, *33*, 115. (d) Daniele, S.; Drost, C.; Gehrhus, B.; Hawkins, S. M.; Hitchcock, P. B.; Lappert, M. F.; Merle, P. G.; Bott, S. G. *J. Chem. Soc., Dalton Trans.* **2001**, 3179. (e) Chivers, T.; Fedorchuk, C.; Parvez, M. *Inorg. Chem.* **2004**, *43*, 2643. (f) Briand, G. G.; Chivers, T.; Parvez, M. *J. Chem. Soc., Dalton Trans.* **2002**, 3785.

(27) (a) Gupta, L. Rate Studies of Organolithium-Mediated Reactions: Reaction of Lithium Diisopropyamide with Fluoropyridines and

Reaction of Lithium Diethylamide with an Alkyl Bromide and an Alkyl Sulfonate. Ph.D. Thesis, Cornell University, Ithaca, NY, 2010. (b) Hoepker, A. C. Aggregation Dynamics of Lithium Diisopropylamide and Their Influence on Reactivity. Ph.D. Thesis, Cornell University, Ithaca, NY, 2011. (c) Zhou, B.; Ma, Y.; Liang, J.; Bruneau, A.; Collum, D. B. Unpublished.

(28) (a) Stegelmann, C.; Andreasen, A.; Campbell, C. T. *J. Am. Chem. Soc.* **2009**, *131*, 8077. (b) Maniscalco, S. J.; Tally, J. F.; Fisher, H. F. *Arch. Biochem. Biophys.* **2004**, *425*, 165. (c) Ruszczycky, M. W.; Anderson, V. E. *J. Theor. Biol.* **2006**, *243*, 328. (d) Ray, W. J., Jr. *Biochemistry* **1983**, *22*, 4625.

(29) Exceedingly fast LDA-mediated reactions are observable by Reich and co-workers using rapid-injection NMR spectroscopy. For leading references to the method, see: Jones, A. C.; Sanders, A. W.; Sikorski, W. H.; Jansen, K. L.; Reich, H. J. *J. Am. Chem. Soc.* **2008**, *130*, 6060.